# Simulating partially coherent fields and other special beam classes in turbulence

Greg Gbur

Department of Physics and Optical Science, University of North Carolina at Charlotte, Charlotte, NC 28223, USA

## ABSTRACT

Optical coherence theory traditionally deals with the properties of randomly fluctuating fields over long time averages. For certain applications (such as optical communications) and special beam classes (such as vortex beams), however, the averaging process can obscure important physical aspects of the field behavior. We demonstrate a new method of simulating partially coherent fields of nearly arbitrary spatial and temporal coherence. Over sufficiently long time intervals, these simulations produce the expected average properties. The results are used to gain insight into the propagation properties of partially coherent fields through atmospheric turbulence.

**Keywords:** coherence, turbulence

## 1. INTRODUCTION

Optical coherence theory is a well-established discipline in optical science which focuses on characterizing the statistical properties and behaviors of randomly fluctuating wavefields. Numerous books have been written on the general theory and applications.[1,2] However, in some significant circumstances the averaging process can mask important aspects of the field behavior. For instance, there is now a wide body of literature which suggests that partially coherent fields are less susceptible to turbulence degradation than their fully coherent counterparts (see, for instance, Refs. [3–9]). This has lead to the possibility of using partially coherent sources for free-space optical communications. The origin of the improvement, however, is still unclear, which implies that systematic optimization of the effect is not yet possible. Furthermore, there are at least three time scales in the problem: the optical period, the coherence time, and the data communication rate. Coherence theory calculations involve a long time average over all three time scales and obscure issues that might arise over finite time intervals. An example of one such issue is beam wander in turbulence.[10]

Other significant field properties can be 'hidden' by the averaging process. For instance, in recent years there has been much interest in beams possessing orbital angular momentum, so-called vortex beams.[11] Optical vortices are characterized by an intensity null at their center and a helical phase front, and they are stable under amplitude and phase perturbations of the field. When the vortex field itself is partially coherent, or its coherence is reduced on propagation through a random medium, the vortex position fluctuates and no point in space will, on average, possess an intensity null, even though the vortex is present at all times in the field. Averaging could be said to be a rather blunt tool for studying vortex behavior; similar statements have been made concerning the use of averaging in the study of laser speckle fields.[12]

The reasons above suggest it would be advantageous in some circumstances to study specific, non-averaged realizations of partially coherent fields with specified average properties. The problem is non-trivial, and most studies of random processes work in the other direction, deriving the average properties from a specified random process (though some exceptions exist[13]). In this article we present a method of generating numerical realizations of a partially coherent field of nearly arbitrary spatial and temporal coherence. The average spectral properties, spatial coherence properties, and intensity profile of the field can be freely and independently chosen. The method is an extension and reimagining of a technique used to study the invariance properties of random fields in dispersive media[14]; it may also be considered an extension of techniques used for studying random electrical noise.[15]

Further author information: E-mail: gjgbur@uncc.edu

In section 2 of the article the field generator is introduced, and results relating to Schell-model sources are developed. In section 3 a modification of the generator is introduced which allows the simulation of fields which consist of a finite number of mutually incoherent modes. In section 4 several examples of partially coherent fields are described, and simulations of their propagation through atmospheric turbulence are presented. Section 5 presents concluding remarks.

## 2. THE PARTIALLY COHERENT FIELD GENERATOR

The partially coherent field generator is introduced as a generalization of the technique used in Ref. 14 to study the propagation of partially coherent fields in dispersive media; in that reference, only one-dimensional wave propagation was considered, and only temporal coherence was considered. As the goal of this article is to generate a realization of a field with specified spatial and temporal coherence properties, we first introduce a model of a partially coherent field which can be implemented numerically; we then determine how the parameters of this model are related to the average properties of the partially coherent field.

We consider a source of partially coherent radiation in the plane $z = 0$, which emits optical pulses of fixed spatial and temporal shape at random times. We initially restrict ourselves to a time interval $t \in [-T/2, T/2]$. Assuming that the pulses are emitted independently of one another, the probability $p(N)$ that $N$ are emitted in this interval is dictated by Poissonian statistics, i.e.

$$p(N) = \frac{\overline{N}^N}{N!} \exp[-\overline{N}]. \tag{1}$$

Let us assume that $N$ pulses are emitted in this interval. The field of these $N$ pulses is then given by

$$V_N(\mathbf{r}, t) = \sum_{j=1}^{N} \Lambda(\mathbf{r}, t - t_j) \exp[-\mathrm{i}\mathbf{K}_j \cdot \mathbf{r}], \tag{2}$$

where $\Lambda(\mathbf{r}, t)$ is the field amplitude of a single pulse in the plane $z = 0$ at transverse position $\mathbf{r} = (x, y)$, aside from a linear phase term, $t_j$ is the time of emission of the $j$th pulse and $\mathbf{K}_j$ is the angle of inclination of the $j$th pulse. The time of arrival is assumed to be a random variable uniformly distributed throughout the interval, and the angle of inclination is a random variable whose probability distribution $P(\mathbf{K})$ is for now unspecified. This representation of the field is very similar to that used in Ref.[14]; however, the introduction of the angle of inclination $\mathbf{K}_j$ and its probability distribution allows us to control the spatial coherence properties of the field as well as the temporal properties.

Once the pulse shape $\Lambda(\mathbf{r}, t)$, the average number of pulses $\overline{N}$ and the probability distribution $P(\mathbf{K})$ are specified, realizations of the field can be generated. We now consider how these quantities are related to the average properties of the field, such as the mutual coherence function.

The mutual coherence function of a statistically stationary field $V(\mathbf{r}, t)$ is defined as

$$\Gamma(\mathbf{r}_1, \mathbf{r}_2, \tau) \equiv \langle V^*(\mathbf{r}_1, t_1) V(\mathbf{r}_2, t_2) \rangle, \tag{3}$$

where $\tau \equiv t_2 - t_1$ and the angle brackets denote ensemble averaging. It is to be noted that this ensemble average is equivalent to three independent averages: the average over the arrival times $t_j$ of the pulses, the average over the inclination factors $\mathbf{K}_j$, and the average over the number of pulses per interval $N$. The instantaneous form of this function for our field of $N$ pulses is

$$V_N^*(\mathbf{r}_1, t_1) V_N(\mathbf{r}_2, t_2) = \sum_{i,j=1}^{N} \Lambda^*(\mathbf{r}_1, t_1 - t_i) \exp[\mathrm{i}\mathbf{K}_i \cdot \mathbf{r}_1] \Lambda(\mathbf{r}_2, t_2 - t_j) \exp[-\mathrm{i}\mathbf{K}_j \cdot \mathbf{r}_2]. \tag{4}$$

We first wish to evaluate the functional form of this quantity when we average over the arrival times $t_i$. To do so, we express $\Lambda(\mathbf{r}, t)$ in terms of its temporal Fourier transform, i.e.

$$\Lambda(\mathbf{r}, t) = \int_0^\infty \tilde{\Lambda}(\mathbf{r}, \omega) e^{-i\omega t} \mathrm{d}\omega. \tag{5}$$

Our expression (4) may then be written in the form

$$V_N^*(\mathbf{r}_1,t_1)V_N(\mathbf{r}_2,t_2)=\sum_{i,j=1}^{N}\int_0^\infty\int_0^\infty \tilde{\Lambda}^*(\mathbf{r}_1,\omega)\tilde{\Lambda}(\mathbf{r}_2,\omega')\exp[\mathrm{i}\mathbf{K}_i\cdot\mathbf{r}_1]\exp[-\mathrm{i}\mathbf{K}_j\cdot\mathbf{r}_2] \\ \times \quad \exp[\mathrm{i}\omega(t_1-t_i)]\exp[-\mathrm{i}\omega'(t_2-t_j)]\mathrm{d}\omega\mathrm{d}\omega'. \tag{6}$$

The time average of a function of $t_i$ and $t_j$ over the interval can be written as

$$\langle F(t_i,t_j)\rangle = \frac{1}{T^2}\int_{-T/2}^{T/2}\int_{-T/2}^{T/2}F(t_i,t_j)\mathrm{d}t_i\mathrm{d}t_j. \tag{7}$$

We may therefore write

$$\langle\exp[-\mathrm{i}(\omega t_i-\omega' t_j)]\rangle = \begin{cases} \mathrm{sinc}[(\omega-\omega')T/2]\equiv f(\omega-\omega'), & i=j, \\ \mathrm{sinc}[\omega T/2]\mathrm{sinc}[\omega' T/2]\equiv g(\omega)g(\omega'), & i\neq j, \end{cases} \tag{8}$$

$$\langle\exp[-\mathrm{i}\omega t_i]\rangle \quad = \quad \mathrm{sinc}[\omega T/2]\equiv g(\omega), \tag{9}$$

where $\mathrm{sinc}[x]\equiv\sin[x]/x$. We may separate our expression (6) into two distinct sums: one for which $i=j$ and one for which $i\neq j$. We may then write

$$\langle V_N^*(\mathbf{r}_1,t_1)V_N(\mathbf{r}_2,t_2)\rangle=\sum_{i=1}^{N}\int_0^\infty\int_0^\infty \tilde{\Lambda}^*(\mathbf{r}_1,\omega)\tilde{\Lambda}(\mathbf{r}_2,\omega')\langle\exp[\mathrm{i}\mathbf{K}_i\cdot(\mathbf{r}_1-\mathbf{r}_2)]\rangle \\ \times \quad \exp[\mathrm{i}(\omega t_1-\omega' t_2)]f(\omega-\omega')\mathrm{d}\omega\mathrm{d}\omega' \\ + \quad \sum_{i\neq j}^{N}\int_0^\infty\int_0^\infty \tilde{\Lambda}^*(\mathbf{r}_1,\omega)\tilde{\Lambda}(\mathbf{r}_2,\omega')\langle\exp[\mathrm{i}(\mathbf{K}_i\cdot\mathbf{r}_1-\mathbf{K}_j\cdot\mathbf{r}_2)]\rangle \\ \times \quad \exp[\mathrm{i}(\omega t_1-\omega' t_2)]g(\omega)g(\omega')\mathrm{d}\omega\mathrm{d}\omega'. \tag{10}$$

At this point, the angle brackets on the exponentials refer only to averaging over the inclination factors $\mathbf{K}_j$. We now use our probability density function to evaluate this average. We have

$$\langle\exp[\mathrm{i}\mathbf{K}_i\cdot(\mathbf{r}_1-\mathbf{r}_2)]\rangle=\int P(\mathbf{K}_i)\exp[\mathrm{i}\mathbf{K}_i\cdot(\mathbf{r}_1-\mathbf{r}_2)]\mathrm{d}^2K_i=(2\pi)^2\tilde{P}(\mathbf{r}_2-\mathbf{r}_1), \tag{11}$$

$$\langle\exp[\mathrm{i}(\mathbf{K}_i\cdot\mathbf{r}_1-\mathbf{K}_j\cdot\mathbf{r}_2)]\rangle=(2\pi)^4\tilde{P}^*(\mathbf{r}_1)\tilde{P}(\mathbf{r}_2), \tag{12}$$

where $\tilde{P}(\mathbf{r})$ represents the two-dimensional Fourier transform of the probability density function, defined by

$$\tilde{P}(\mathbf{r}) = \frac{1}{(2\pi)^2}\int P(\mathbf{K})\exp[-\mathrm{i}\mathbf{K}\cdot\mathbf{r}]\mathrm{d}^2K. \tag{13}$$

The sums may then be evaluated, and we find that

$$\begin{aligned} \Gamma_N(\mathbf{r}_1,\mathbf{r}_2,\tau) \quad &= \quad \langle V_N^*(\mathbf{r}_1,t_1)V_N(\mathbf{r}_2,t_2)\rangle \\ &= \quad (2\pi)^2 N\int_0^\infty\int_0^\infty \tilde{\Lambda}^*(\mathbf{r}_1,\omega)\tilde{\Lambda}(\mathbf{r}_2,\omega')\tilde{P}(\mathbf{r}_2-\mathbf{r}_1) \\ &\times \quad \exp[\mathrm{i}(\omega t_1-\omega' t_2)]f(\omega-\omega')\mathrm{d}\omega\mathrm{d}\omega' \\ &+ \quad (2\pi)^4 N(N-1)\int_0^\infty\int_0^\infty \tilde{\Lambda}^*(\mathbf{r}_1,\omega)\tilde{\Lambda}(\mathbf{r}_2,\omega')\tilde{P}^*(\mathbf{r}_1)\tilde{P}(\mathbf{r}_2) \\ &\times \quad \exp[\mathrm{i}(\omega t_1-\omega' t_2)]g(\omega)g(\omega')\mathrm{d}\omega\mathrm{d}\omega'. \end{aligned} \tag{14}$$

At this point the integrals are completely independent of the individual realizations of pulses, i.e. the particular values of $t_j$ and $\mathbf{K}_j$ for each pulse, and the only random variable remaining is the number of pulses in the interval. We may average over this quantity as well, to get the mutual coherence function as

$$\Gamma(\mathbf{r}_1, \mathbf{r}_2, \tau) = \sum_{N=0}^{\infty} p(N)\Gamma_N(\mathbf{r}_1, \mathbf{r}_2, \tau), \tag{15}$$

where $p(N)$ is the Poisson distribution. We need the well-established results

$$\sum_{N=0}^{\infty} p(N)N = \overline{N}, \tag{16}$$

$$\sum_{N=0}^{\infty} p(N)N(N-1) = \overline{N}^2. \tag{17}$$

The mutual coherence function may then be written as

$$\begin{aligned}
\Gamma(\mathbf{r}_1, \mathbf{r}_2, \tau) &= (2\pi)^2\overline{N}\int_0^{\infty}\int_0^{\infty} \tilde{\Lambda}^*(\mathbf{r}_1, \omega)\tilde{\Lambda}(\mathbf{r}_2, \omega')\tilde{P}(\mathbf{r}_2 - \mathbf{r}_1) \\
&\times \exp[\mathrm{i}(\omega t_1 - \omega' t_2)]f(\omega - \omega')\mathrm{d}\omega\mathrm{d}\omega' \\
&+ (2\pi)^4\overline{N}^2\int_0^{\infty}\int_0^{\infty} \tilde{\Lambda}^*(\mathbf{r}_1, \omega)\tilde{\Lambda}(\mathbf{r}_2, \omega')\tilde{P}^*(\mathbf{r}_1)\tilde{P}(\mathbf{r}_2) \\
&\times \exp[\mathrm{i}(\omega t_1 - \omega' t_2)]g(\omega)g(\omega')\mathrm{d}\omega\mathrm{d}\omega'.
\end{aligned} \tag{18}$$

Defining the average rate of pulse emission as $\eta = \overline{N}/T$, we may rewrite Eq. (18) in the form

$$\begin{aligned}
\Gamma(\mathbf{r}_1, \mathbf{r}_2, \tau) &= (2\pi)^2\eta\int_0^{\infty}\int_0^{\infty} \tilde{\Lambda}^*(\mathbf{r}_1, \omega)\tilde{\Lambda}(\mathbf{r}_2, \omega')\tilde{P}(\mathbf{r}_2 - \mathbf{r}_1) \\
&\times \exp[\mathrm{i}(\omega t_1 - \omega' t_2)]f(\omega - \omega')T\mathrm{d}\omega\mathrm{d}\omega' \\
&+ (2\pi)^4\eta^2\int_0^{\infty}\int_0^{\infty} \tilde{\Lambda}^*(\mathbf{r}_1, \omega)\tilde{\Lambda}(\mathbf{r}_2, \omega')\tilde{P}^*(\mathbf{r}_1)\tilde{P}(\mathbf{r}_2) \\
&\times \exp[\mathrm{i}(\omega t_1 - \omega' t_2)]g(\omega)Tg(\omega')T\mathrm{d}\omega\mathrm{d}\omega'.
\end{aligned} \tag{19}$$

Letting the measurement interval $T \to \infty$, the functions $f(\omega)T$ and $g(\omega)T$ reduce to

$$f(\omega - \omega')T \to 2\pi\delta(\omega - \omega'), \tag{20}$$

$$g(\omega) \to 4\pi\delta^{(e)}(\omega), \tag{21}$$

where $\delta(\omega)$ is the Dirac delta function and $\delta^{(e)}$ is the even half-delta function, defined such that

$$\int_0^{\epsilon} \delta^{(e)}(\omega)\mathrm{d}\omega = \frac{1}{2}. \tag{22}$$

By use of these results, the mutual coherence function becomes

$$\begin{aligned}
\Gamma(\mathbf{r}_1, \mathbf{r}_2, \tau) &= (2\pi)^3\eta\int_0^{\infty} \tilde{\Lambda}^*(\mathbf{r}_1, \omega)\tilde{\Lambda}(\mathbf{r}_2, \omega)\tilde{P}(\mathbf{r}_2 - \mathbf{r}_1)\exp[-\mathrm{i}\omega\tau]\mathrm{d}\omega \\
&+ (2\pi)^6\eta^2\tilde{\Lambda}^*(\mathbf{r}_1, 0)\tilde{\Lambda}(\mathbf{r}_2, 0)\tilde{P}^*(\mathbf{r}_1)\tilde{P}(\mathbf{r}_2).
\end{aligned} \tag{23}$$

The latter term is the DC-contribution to the field. If we are considering sufficiently narrowband optical signals, it may be safely neglected.

One more simplification will be convenient. We assume that the spatial and temporal parts of the field factorize, i.e. that

$$\Lambda(\mathbf{r}, t) = \Theta(\mathbf{r})\Phi(t), \tag{24}$$

so that

$$\tilde{\Lambda}(\mathbf{r},\omega) = \Theta(\mathbf{r})\tilde{\Phi}(\omega). \tag{25}$$

We may then write

$$\Gamma(\mathbf{r}_1,\mathbf{r}_2,\tau) = \eta(2\pi)^3\Theta^*(\mathbf{r}_1)\Theta(\mathbf{r}_2)\tilde{P}(\mathbf{r}_2-\mathbf{r}_1)\int_0^\infty |\tilde{\Phi}(\omega)|^2\exp[-\mathrm{i}\omega\tau]\mathrm{d}\omega. \tag{26}$$

If we consider this field in the space-frequency domain, and consider instead the cross-spectral density $W(\mathbf{r}_1,\mathbf{r}_2,\omega)$ of the field, we have

$$W(\mathbf{r}_1,\mathbf{r}_2,\omega) = \eta(2\pi)^3|\tilde{\Phi}(\omega)|^2\Theta^*(\mathbf{r}_1)\Theta(\mathbf{r}_2)\tilde{P}(\mathbf{r}_2-\mathbf{r}_1), \tag{27}$$

where

$$W(\mathbf{r}_1,\mathbf{r}_2,\omega) = \frac{1}{2\pi}\int_{-\infty}^{\infty}\Gamma(\mathbf{r}_1,\mathbf{r}_2,\tau)\exp[\mathrm{i}\omega\tau]\mathrm{d}\tau. \tag{28}$$

Equation (27) is the main result of this article. It demonstrates that the cross-spectral density of our realization of pulses will have a spectrum $|\tilde{\Phi}(\omega)|^2$, an average field profile $\Theta^*(\mathbf{r}_1)$ and a spectral degree of coherence $\tilde{P}(\mathbf{r}_2-\mathbf{r}_1)$. These three functions can be chosen independently of one another, and we may therefore construct a realization of a partially coherent field which has quite general spatial and temporal coherence.

It is to be noted that our results are not completely general, i.e. there exist partially coherent fields which cannot be realized by this random pulse technique. In particular, there exist fields whose spatial and temporal coherence properties are not factorizable, and there also exist fields whose spectral degree of coherence is frequency dependent. Nevertheless, our method provides an excellent tool for creating realizations of quite arbitrary spatial and temporal coherence.

## 3. MODIFYING THE GENERATOR FOR MODAL EXPANSIONS

It is often convenient to express the cross-spectral density of a partially coherent field in a modal expansion of the form

$$W(\mathbf{r}_1,\mathbf{r}_2,\omega) = \sum_{n=1}^{N}\lambda_n(\omega)\phi_n^*(\mathbf{r}_1,\omega)\phi_n(\mathbf{r}_2,\omega). \tag{29}$$

In this formula, $\lambda_n(\omega) > 0$ and the functions $\phi_n(\mathbf{r},\omega)$ are the *modes* of the field. The index $n$ may represent multiple indices and there may be an infinite number of modes. If, in the source plane $z = 0$, these modes are mutually orthonormal, i.e.

$$\iint_{-\infty}^{\infty}\phi_n^*(\mathbf{r}',\omega)\phi_m(\mathbf{r}',\omega)d^2r' = \delta_{mn}\lambda_n(\omega), \tag{30}$$

where $\delta_{mn}$ is the Kroenecker delta, the modal expansion is referred to as a *coherent mode expansion*[16] and can be shown to be unique. The modes can be seen to be mutually incoherent by considering the spectral density of the field,

$$S(\mathbf{r},\omega) = W(\mathbf{r},\mathbf{r},\omega) = \sum_{n=1}^{N}\lambda_n(\omega)|\phi_n(\mathbf{r},\omega)|^2.$$

Simple partially coherent sources can be created by combining a finite number of modes into a single beam. It was recently shown[17] that an appreciable reduction of scintillation can be achieved by the use of two independent Gaussian beams with different wavelengths.

Such modal fields, however, are not in general Schell-model, and the analysis of the previous section cannot be applied to them without some modification. In this section we demonstrate how this can be done.

We consider a field of the form

$$V_{N,M}(\mathbf{r},t) = \sum_{i=1}^{N}\Lambda_1(\mathbf{r},t-t_i) + \sum_{\alpha=1}^{M}\Lambda_2(\mathbf{r},t-t_\alpha), \tag{31}$$

where $\Lambda_k$, $k = 1, 2$ are different field amplitudes. The instantaneous form of the mutual coherence function can be written as

$$V^*_{N,M}(\mathbf{r}_1, t_1)V_{N,M}(\mathbf{r}_2, t_2) = \left[\sum_{i=1}^{N} \Lambda_1(\mathbf{r}, t - t_i) + \sum_{\alpha=1}^{M} \Lambda_2(\mathbf{r}, t - t_\alpha)\right]^* \left[\sum_{j=1}^{N} \Lambda_1(\mathbf{r}, t - t_j) + \sum_{\beta=1}^{M} \Lambda_2(\mathbf{r}, t - t_\beta)\right]. \quad (32)$$

The time average over the interval $[-T/2, T/2]$ can be carried out as in the previous section by Fourier expanding the temporal pulse envelopes and using Eqs. (8) and (9), noting that the times labelled by Roman and Greek subscripts are independent. Furthermore, we assume that the number of pulses of type 1 and type 2 are each dictated by their own Poisson distribution, with average rates $\eta_1$ and $\eta_2$. Averaging over pulse number and letting the measurement interval $T \to \infty$, we readily find that

$$\begin{aligned} \Gamma(\mathbf{r}_1, \mathbf{r}_2, \tau) &= (2\pi)\eta_1 \int_0^\infty \tilde{\Lambda}^*_1(\mathbf{r}_1, \omega)\tilde{\Lambda}_1(\mathbf{r}_2, \omega) \exp[-i\omega\tau]d\omega + (2\pi)\eta_2 \int_0^\infty \tilde{\Lambda}^*_2(\mathbf{r}_1, \omega)\tilde{\Lambda}_2(\mathbf{r}_2, \omega) \exp[-i\omega\tau]d\omega \\ &+ \text{DC-terms.} \end{aligned} \quad (33)$$

If we again assume that the spatial and temporal parts of each pulse factorize, i.e.

$$\Lambda_i(\mathbf{r}, t) = \Theta_i(\mathbf{r})\Phi_i(t), \quad (34)$$

and neglect the DC-components, we may write the cross-spectral density of the field as

$$W(\mathbf{r}_1, \mathbf{r}_2, \omega) = (2\pi)\eta_1|\tilde{\Phi}_1(\omega)|^2\Theta^*_1(\mathbf{r}_1)\Theta_1(\mathbf{r}_2) + (2\pi)\eta_2|\tilde{\Phi}_2(\omega)|^2\Theta^*_2(\mathbf{r}_1)\Theta_2(\mathbf{r}_2). \quad (35)$$

This cross-spectral density has the form of a field with two modes, as a special case of Eq. (29). By adding additional independent pulse shapes to the simulation (i.e. $\Lambda_3$, $\Lambda_4$, etc.), we may generate realizations of partially coherent fields with an arbitrary finite number of modes.

## 4. EXAMPLES

We now demonstrate the use of the field generator by numerical examples.

### 4.1. Gaussian Schell-model fields

We consider fields of Gaussian intensity profile and Gaussian spatial correlation, known as Gaussian Schell-model fields (Ref. [2], Sec. 5.2.2.). The mutual coherence function of such fields may be written as

$$\Gamma(\mathbf{r}_1, \mathbf{r}_2, \tau) = \gamma(\tau)\sqrt{I(\mathbf{r}_1)}\sqrt{I(\mathbf{r}_2)}\mu(\mathbf{r}_2 - \mathbf{r}_1), \quad (36)$$

where $I(\mathbf{r})$ is the average field intensity,

$$I(\mathbf{r}) = \exp[-\mathbf{r}^2/2\sigma_I^2], \quad (37)$$

$\sigma_I$ being the beam width, $\mu(\mathbf{r}_2 - \mathbf{r}_1)$ is the spatial correlation function (equivalent to the spectral degree of coherence in the frequency domain),

$$\mu(\mathbf{r}_2 - \mathbf{r}_1) = \exp[-(\mathbf{r}_2 - \mathbf{r}_1)^2/2\sigma_g^2], \quad (38)$$

$\sigma_g$ being the correlation length, and $\gamma(\tau)$ is the temporal coherence function, to be taken as Lorentzian or Gaussian. On comparison with Eq. (27), it can be seen that our field generator should generate a Gaussian Schell-model field if we take $\sqrt{I(\mathbf{r})} = \sqrt{\eta(2\pi)^3}\Theta(\mathbf{r})$, $\tilde{P}(\mathbf{r}) = \mu(\mathbf{r})$, and take $|\tilde{\Phi}(\omega)|^2$ to be the temporal Fourier transform of $\gamma(\tau)$. Figure 1 illustrates the intensity of the field generated by our simulation method for several realizations, with $\sigma_I = 2\,\text{cm}$, $\sigma_g = 1\,\text{cm}$, and Gaussian spectrum of center frequency $1 \times 10^{15}\,\text{Hz}$ and 1% bandwidth. The average pulse rate is taken to be 5 pulses/cycle. The pictures show the gradual evolution of the field in time; the frames are each separated by 5 periods at the center frequency.

To be a valid technique for generating realizations, the field must possess the proper prescribed average properties. Figure 2 illustrates the average intensity of the field, taken over 50 instantaneous values of the field

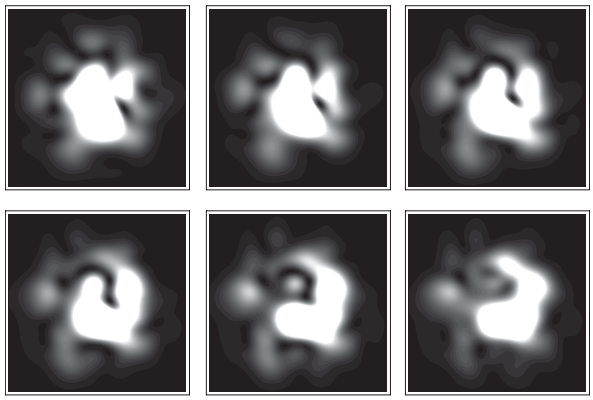

**Figure 1.** Illustrating several realizations of the intensity of the field generated by the method with $\sigma_I = 2\,\text{cm}$, $\sigma_g = 1\,\text{cm}$, and Gaussian spectrum of center frequency $1 \times 10^{15}\,\text{Hz}$ and 1% bandwidth. The pictures show the gradual evolution of the field in time; the frames are each separated by 5 periods at the center frequency. The window size is 10 cm on a side.

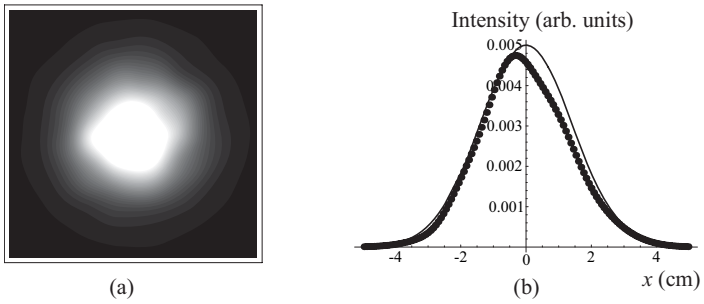


**Figure 2.** Illustrating the average intensity of the field (a) in the source plane and (b) through a cross-section of the source plane. The dots indicate the numerically calculated result; the solid line indicates the expected result of Eq. (36). The average is taken over 50 instantaneous values of the field, each separated by 20 periods at the center frequency. All other parameters are as in Fig. 1.

each separated by 20 periods at the center frequency. Part (a) shows the cross-section of the beam, while (b) shows the cross-section of the beam along the line $y = 0$. The ideal Gaussian is shown as a dashed line, and it can be seen that there is excellent agreement. Convergence could be further improved by extending the duration of the time average.

The spatial correlation properties can also be numerically calculated to test the technique. Figure 3 shows the average spatial correlation properties, taken over 50 instantaneous values of the field each separated by 20 periods at the center frequency. The spatial correlation properties were calculated at points $+x$, $-x$ along the line $y = 0$. The circles represent the results generated from our realization, while the dashed line represents the ideal Gaussian Schell-model case. Again it can be seen that there is excellent agreement.

The average temporal correlation properties of the field can also be numerically calculated. Figure 4 shows the complex degree of coherence $\gamma(\tau)$ calculated at the center of a coherent Gaussian beam, for a Gaussian and Lorentian lineshape. Again there is excellent agreement between the results of the simulation and the expected average behavior.

### 4.2. Modal fields in atmospheric turbulence

We now consider the propagation of a two-mode field through atmospheric turbulence. The modes are taken to be asymmetric Gaussian beams of the form

$$I(\mathbf{r}) = \exp[-x^2/2\sigma_x^2] \exp[-y^2/2\sigma_y^2].$$

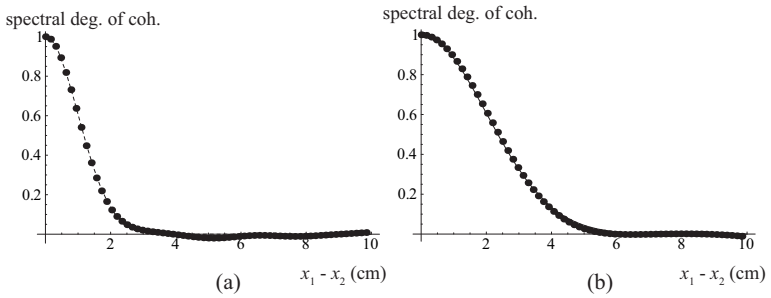


**Figure 3.** Illustrating the spectral degree of coherence of the field as calculated using 50 instantaneous values of the field, each separated by 20 periods at the center frequency. For (a), $\sigma_g = 1\,\text{cm}$, while for (b), $\sigma_g = 2\,\text{cm}$. The dashed lines indicate the expected result of Eq. (36).

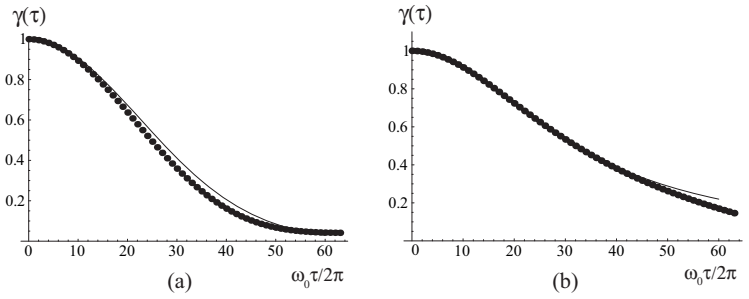


**Figure 4.** Illustrating the temporal coherence function calculated by time averaging. The solid lines indicate the analytic prediction. For (a), the function is Gaussian, while for (b), the function is Lorentzian.

For mode 1, we use $\omega_1 = 1.00 \times 10^{15}\,\text{Hz}$ and 1% bandwidth, with $\sigma_x = 2\,\text{cm}$ and $\sigma_y = 3\,\text{cm}$, while for mode 2, $\omega_2 = 1.01 \times 10^{15}\,\text{Hz}$ and 1% bandwidth, with $\sigma_x = 3\,\text{cm}$ and $\sigma_y = 2\,\text{cm}$. The partially coherent field is propagated through turbulence with a von Karman spectrum[10] with $C_n^2 = 10^{-15}\,\text{m}^{-2/3}$, inner scale $l_0 = 1\,\text{mm}$ and outer scale $L_0 = 1\,\text{m}$, and the turbulence is simulated numerically by the use of multiple phase screens.[18]

Figure 5(a) illustrates a number of images at a detector plane situated 3 km from the source, each separated by 5 cycles of the field at frequency $\omega_1$. Although on average we expect the fields to be independent of one another, instantaneously one mode or the other may be dominant, or some complicated interference pattern may arise from their interaction. Only on average (shown in Fig. 5(b)) do we get a somewhat regular, circular spot. These figures illustrate that the behavior of the field will be appreciably different on short time scales, and this will ultimately effect the maximum data communication rate possible for partially coherent laser fields in turbulence.

The modal picture of partially coherent field propagation in turbulence suggests the following picture for the improved propagation characteristics of partially coherent fields in turbulence, as illustrated in Fig. 6. A coherent laser essentially propagates its energy through a single coherent mode, which is subject to distortion on propagation through the inhomogeneous medium. The signal may or may not arrive fully at the detector, and will have suffered degradation due to diffraction. The partially coherent beam sends its energy through multiple (independent) modes, each of which propagates differently in the turbulent medium. Although any individual mode may not arrive cleanly at the detector, it is likely that at least one will make the journey.

## 5. CONCLUSIONS

We have derived a new method of generating realizations of partially coherent fields of nearly arbitrary spatial and temporal coherence. The method was derived for both Schell-model fields of different degrees of spatial and temporal coherence as well as for modal fields of a finite number of modes. The numerically calculated average properties agree well with the predicted analytical results. The method was also used to gain some

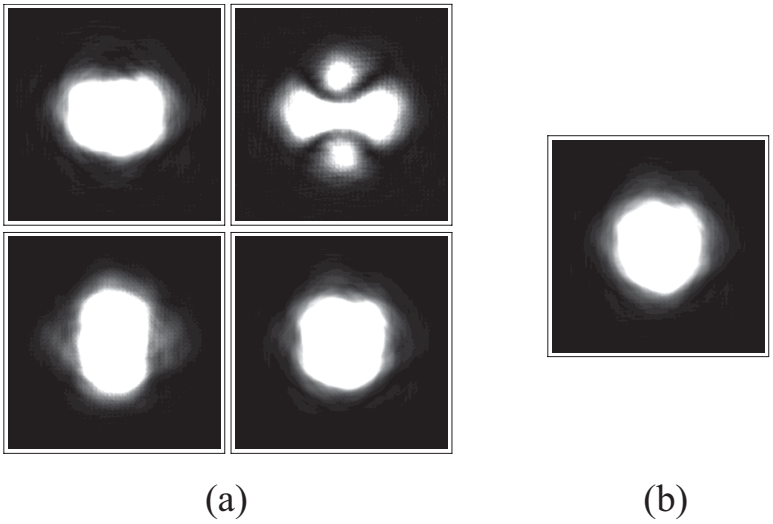


**Figure 5.** (a) Snapshots of the field intensity at the detector, at intervals separated by 5 cycles of the center frequency $\omega_1$. The plots are 50 cm on a side. (b) The average field intensity at the detector, calculated over 25 snapshots.

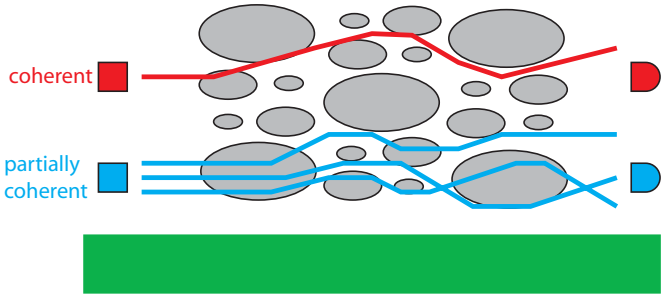


**Figure 6.** A qualitative explanation of the behavior of partially coherent beams in turbulence. A coherent laser essentially propagates its energy through a single coherent mode, which is subject to distortion on propagation through the inhomogeneous medium. The partially coherent beam sends its energy through multiple (independent) modes, each of which propagates differently in the turbulent medium.

insight into the propagation of partially coherent beams through atmospheric turbulence. It is expected that the ability to study the behavior of fluctuating fields on many time scales (center frequency, bandwidth, rate of turbulence fluctuations, detector response) will provide useful insight into the behaviors of many coherence-related phenomena.

## ACKNOWLEDGMENTS

The research was supported by the US Air Force Office of Scientific Research under grant FA 9550-05-1-0288.

## REFERENCES

1. M. Born and E. Wolf, *Principles of Optics*, Cambridge University Press, Cambridge, 1999 (seventh expanded edition).
2. L. Mandel and E. Wolf, *Optical Coherence and Quantum Optics*, Cambridge University Press, Cambridge, 1995.
3. J. C. Leader, "Atmospheric propagation of partially coherent radiation," *J. Opt. Soc. Am.* **68**, pp. 175–185, 1978.
4. R. Fante, "Intensity fluctuations of an optical wave in a turbulent medium: effect of source coherence," *Optica Acta* **28**, pp. 1203–1207, 1981.
5. J. Wu, "Propagation of a Gaussian-Schell beam through turbulent media," *J. Mod. Opt.* **37**, pp. 671–684, 1990.
6. J. Wu and A. D. Boardman, "Coherence length of a Gaussian Schell-model beam and atmospheric turbulence," *J. Mod. Opt.* **38**, pp. 1355–1363, 1991.
7. G. Gbur and E. Wolf, "Spreading of partially coherent beams in random media," *J. Opt. Soc. Am. A* **19**, pp. 1592–1598, 2002.
8. J. C. Ricklin and F. M. Davidson, "Atmospheric turbulence effects on a partially coherent Gaussian beam: implications for free-space laser communication," *J. Opt. Soc. Am. A* **19**, pp. 1794–1802, 2002.
9. L. C. A. O. Korotkova and R. L. Phillips, "A model for a partially coherent Gaussian beam in atmospheric turbulence with application in lasercom," *Opt. Eng.* **43**, pp. 330–341, 2004.
10. L. Andrews and R. Phillips, *Laser Beam Propagation through Random Media*, SPIE Press, Bellingham, Washington, 1998.
11. M. Soskin and M. Vasnetsov, "Singular optics," *Progress in Optics* **42**, pp. 219–276, Elsevier, Amsterdam, 2001.
12. I. Freund, "'1001' correlations in random wave fields," *Waves in Random Media* **8**, pp. 119–158, 1998.
13. E. K. B. Davis and J. R. Piepmeier, "Stochastic modeling and generation of partially polarized or partially coherent electromagnetic waves," *Radio Sci.* **39**, p. RS1001, 2004.
14. W. Wang and E. Wolf, "Invariance properties of random pulses and of other random fields in dispersive media," *Phys. Rev. E* **52**, pp. 5532–5539, 1995.
15. S. Rice, "Mathematical analysis of random noise," in *Selected Papers on Noise and Stochastic Processes*, N. Wax, ed., pp. 219–276, Dover, NY, 1954.
16. E. Wolf, "New theory of partial coherence in the space-frequency domain: Part I: Spectra and cross-spectra of steady-state sources," *J. Opt. Soc. Amer.* **72**, pp. 343–351, 1982.
17. A. Peleg and J. Moloney, "Scintillation index for two Gaussian laser beams with different wavelengths in weak atmospheric turbulence," *J. Opt. Soc. Amer. A* **23**, pp. 3114–3122, 2006.
18. J. M. Martin and S. M. Flatté, "Intensity images and statistics from numerical simulation of wave propagation in 3-D random media," *Appl. Opt.* **27**, pp. 2111–2126, 1988.